Internal Methyl Rotation in the CH Stretching Overtone Spectra of Toluene-α-d_2, -α-d_1, and -d_0

Henrik G. Kjaergaard* and Zimei Rong

Department of Chemistry, University of Otago, P.O. Box 56, Dunedin, New Zealand

Allan J. McAlees, Daryl L. Howard, and Bryan R. Henry*

Department of Chemistry and Biochemistry, University of Guelph, Guelph, Ontario N1G 2W1, Canada

Received: February 11, 2000; In Final Form: May 11, 2000

The room-temperature vapor phase overtone spectrum of toluene-α-d_2 has been recorded in the CH stretching region corresponding to $\Delta v_{CH} = 2-6$ with conventional near-infrared spectroscopy ($\Delta v_{CH} = 2-4$) and with intracavity titanium:sapphire and dye laser photoacoustic spectroscopy ($\Delta v_{CH} = 4-6$). Both absolute oscillator strengths (conventional spectra) and relative oscillator strengths within a given overtone (conventional and photoacoustic spectra) have been measured. The aryl region of the spectrum is interpreted in terms of two nonequivalent aryl local modes and is essentially identical to the aryl regions of the spectra of toluene-d_0 and toluene-α-d_1. However, the methyl band profile differs significantly in these three molecules. We use an anharmonic oscillator local mode model and an ab initio dipole moment function to calculate oscillator strengths for the aryl and methyl transitions. Parameters for this model come from a fit of the aryl transition energies and from a fit of the methyl spectral profiles. These simple calculations give values that are in good agreement with observed absolute and relative intensities. Differences in the methyl profiles in toluene-d_0, -α-d_1, and -α-d_2 are ascribed to coupling between CH stretching and methyl torsional modes. The methyl profiles are simulated on the basis of a simple adiabatic model that incorporates the harmonically coupled anharmonic oscillator local mode approach and our intensity calculations. The model successfully accounts for the change in methyl profiles between the three molecules, demonstrates the importance of torsional stretching coupling, and shows that coupling between the CH stretching oscillators is unimportant for higher overtones ($\Delta v_{CH} \geq 4$).

Introduction

In our previous work on the overtone spectra of toluene-α-d_1[1] and toluene-d_0,[2] we found an interesting result. Whereas the aryl CH stretching region of the spectrum was identical for both molecules, there was a marked change in the methyl spectral profile. We measured absorption intensities in the range of $\Delta v_{CH} = 2-6$. Oscillator strengths were calculated with an approach that used the harmonically coupled anharmonic oscillator (HCAO) local mode model[3−8] to obtain the vibrational wave functions and ab initio theory to obtain the dipole moment functions.[9−12] These intensity calculations showed good agreement between the observed and calculated values for absolute total intensities, for relative intensities, and for the changes in intensities between the two molecules. However, no quantitative attempt was made to account for the change in methyl profile between toluene-d_0 and toluene-α-d_1.

In a molecule with a relatively high barrier to methyl rotation such as dimethyl ether, the methyl group exists in a single preferred conformation. The two conformationally distinct methyl CH bonds, two out-of-plane and one in-plane, differ in bond length. This bond length difference is reflected in two distinct peaks in the overtone spectrum.[13] However, for molecules with a low barrier to methyl rotation such as toluene, the methyl peak is broad[2,14,15] and any spectral structure appears to be unrelated to molecular geometry.

Cavagnat et al.[16] have simulated the methyl profiles from $\Delta v_{CH} = 1-6$ in the spectrum of dideuterionitromethane (NO_2CHD_2). They have also used their model to simulate the methyl profile in the spectrum of monohydrogenated toluene (toluene-α-d_2) in the region of $\Delta v_{CH} = 1-3$.[17] Their model considers the coupling between CH stretching and methyl rotation within the adiabatic approximation. They use a vibrational wave function expressed in terms of anharmonic Morse oscillator wave functions and an ab initio dipole moment function expanded in both CH stretching coordinates and torsional angles. They obtain good agreement between the predictions of their model and their experimental spectra for both molecules.[16,17] They have successfully generalized their model for nitromethane (NO_2CH_3) to include all three methyl CH bonds and vibrational coupling between them.[18] They conclude from their analysis that CH stretching is localized for $\Delta v_{CH} \geq 4$ in the sense that the barrier to methyl group rotation increases markedly for excited vibrational states and is essentially determined by the vibrational energy contribution.[17,18]

A similar approach has been used by Zhu et al.[19] to calculate the methyl profiles of 2,6-difluorotoluene in the regions of $\Delta v_{CH} = 2-6$. In this molecule there is a small barrier to methyl rotation (~46 cm^{-1} compared to ~5 cm^{-1} in toluene) but the methyl torsional motion is relatively free. The model by Zhu et al.[19] includes all three CH bonds of the methyl group. It successfully predicts the methyl overtone spectral profiles and attributes these profiles to a large number of transitions that arise from terms involving torsion−stretch coupling both in the Hamiltonian and in the dipole moment function.

10.1021/jp000571d CCC: $19.00
Published on Web 07/06/2000

Recently, we have measured the overtone spectra of 2-, 3-, and 4-methylpyridine in the region of $\Delta v_{CH} = 2-6$.[20] In these three molecules both the type of barrier (V_3 or V_6) and the height of the barrier changes. In 2-methylpyridine the increased barrier height leads to a change in the methyl profile relative to the other two molecules whose methyl profiles are similar and similar to those of toluene. In another recent study of the molecule neopentane,[21] the width of the methyl spectral profile appears to be affected by through space interaction with other methyl groups within the same molecule for $\Delta v_{CH} \geq 5$.

In this paper we extend our previous work on toluene-d_0 and toluene-α-d_1 to toluene-α-d_2 and simulate the methyl profiles in all three molecules. In our simulations, we will be particularly interested in whether we are able to predict the differences observed in the experimental methyl spectral profiles. Through analysis of these differences, we hope to understand the basis of the couplings that are manifested in the spectra of a wide variety of molecules with methyl substituents.

Experimental Section

Toluene-α-d_2 was prepared following the method of Cavagnat and Lascombe.[22] The isotopic purity was obtained from a 400 MHz ^{1}H NMR spectrum. Integration of the aryl and methyl peaks led to an aryl:methyl ratio of 5.0000:1.0032 in agreement with the expected ratio of 5:1. Given the errors in integration, we estimate the purity of toluene-α-d_2 to be >99%.

The room-temperature vapor phase overtone spectrum of toluene-α-d_2 was recorded in the $\Delta v_{CH} = 2-4$ regions with conventional absorption spectroscopy and in the $\Delta v_{CH} = 4-6$ regions by intracavity laser photoacoustic spectroscopy (ICL-PAS). The conventional spectra were recorded with a Cary 5e that was fitted with a variable path length Wilks cell. Background scans with an evacuated cell were recorded and subtracted for each of the Cary spectra. The experimental absolute oscillator strength f of an absorption band can be determined from these conventional spectra and the equation[23]

$$f = 2.6935 \times 10^{-9}[\mathrm{K}^{-1}\ \mathrm{Torr\ m\ cm}]\frac{T}{pl}\int A(\tilde{\nu})\,\mathrm{d}\tilde{\nu} \qquad (1)$$

where T is the temperature, p is the pressure, l is the path length, A is the absorbance, and $\tilde{\nu}$ is the frequency in cm^{-1}.

Our version of ICL-PAS has been described elsewhere.[24,25] The photoacoustic cell contained an electret microphone (Knowles Electronics Inc., EK3132). In the ICL-PAS spectra, a small amount of argon buffer gas (88−97 Torr) was added to the photoacoustic cell to improve the photoacoustic signal. An argon ion pumped titanium:sapphire solid-state broad band tunable laser with midwave and short-wave optics was used to record the $\Delta v_{CH} = 4$ and 5 regions, respectively. The spectrum of the $\Delta v_{CH} = 6$ region was recorded with the dye R6G, but the methyl region had a relatively low signal-to-noise ratio. The dye DCM yields a better S/N in the methyl region, so the R6G and DCM spectra were spliced together for optimum S/N.

The overtone spectra were decomposed into component peaks with a deconvolution program within Spectra Calc.[26] The spectra were deconvoluted into a number of Lorentzian peaks and a linear baseline. Uncertainty in well-resolved peaks, such as the aryl peaks of toluene-α-d_2, is typically less than 5 cm^{-1} and less than 10% for intensities. The high noise level in the Cary spectrum at $\Delta v_{CH} = 4$ introduces additional error. Deconvolution of the broad methyl band leads to larger uncertainties. We estimate the error in the methyl area to be less than 30% where much of the error arises from uncertainty in the baseline.

Theory and Calculations

The theoretical models that we have used for the intensity calculations in the present paper are similar to the models we used in our previous work on toluene-d_0[2] and -α-d_1.[1] In this paper we also carry out simulations of methyl band profiles and the approach that we have used is similar to that used in our previous work on 2,6-difluorotoluene.[19] Thus, only a brief outline is given here with an indication of changes and reference to previous papers for additional details. The oscillator strength f_{eg} of a vibrational transition from the ground-state g to an excited-state e is given by[23]

$$f_{eg} = 4.702 \times 10^{-7}[\mathrm{cm\ D}^{-2}]\tilde{\nu}_{eg}|\vec{\mu}_{eg}|^2 \qquad (2)$$

where $\tilde{\nu}_{eg}$ is the vibrational wavenumber of the transition and $\vec{\mu}_{eg} = \langle e|\vec{\mu}|g\rangle$ is the transition dipole moment matrix element in Debye (D). Thus, to calculate vibrational band intensities and to simulate methyl band profiles we need to obtain both vibrational wave functions and the dipole moment function.

We have used an axis system with the z-axis along the C−C bond around which the methyl group rotates, and that is positive in the direction of the α-hydrogens. The x-axis is in the plane of the ring and the y-axis is perpendicular to the plane. The positive x-axis direction is toward the aryl CH bond in the 2-position. The internal rotation (torsion) of the methyl group is defined by the torsional angle, θ, which is the dihedral angle between one α-CH bond and the x-axis. The conformer with an α-CH bond parallel (||) to the x-axis ($\theta = 0°$) is a local extreme on the potential energy curve, whereas the conformer with an α-CH bond perpendicular (⊥) to the x-axis ($\theta = 90°$) is another. This axis system is in agreement with that of our previous papers.[1,2,19] The torsional barrier is only 4.9 cm^{-1}, as determined by microwave spectroscopy,[27] and the lowest energy conformer is not conclusively determined.

Vibrational Model. We have used the HCAO local mode model to obtain the vibrational wave functions and energies of the aryl and methyl CH bonds, and a rigid rotor approach for the methyl torsional modes. The coupling between CH bonds attached to different C atoms is very small.[9,12] Thus, the aryl CH bonds can, to a very good approximation, be described by an isolated anharmonic Morse oscillator Hamiltonian[1]

$$(H - E_{|0\rangle_j})/hc = v_j\tilde{\omega}_j - (v_j^2 + v_j)\tilde{\omega}_j x_j \qquad (3)$$

where $E_{|0\rangle_j}$ is the energy of the vibrational ground state and $\tilde{\omega}_j$ and $\tilde{\omega}_j x_j$ are the local mode frequency and anharmonicity of the CH$_j$ oscillator. The eigenstates of an aryl CH oscillator described by eq 3 are simply Morse oscillator wave functions and are denoted by $|v_j\rangle_j$, where v_j is the vibrational quantum number for the CH$_j$ oscillator. The $\tilde{\omega}_j$ and $\tilde{\omega}_j x_j$ parameters were taken from experiment. The ⊥ conformer will have three nonequivalent aryl CH bonds (o, m, p), whereas the || conformer has five (2, 3, 4, 5, 6). However, the aryl CH bonds change very little upon methyl rotation,[2] and on the basis of the calculated CH bond lengths, we would expect two peaks in the aryl region of the overtone spectra of the toluenes in agreement with observations in previous and present spectra. The lower frequency aryl peak is assigned to the CH$_o$ bonds in the ⊥ conformer (or 2- and 6-position for the || conformer), and the higher frequency peak to the CH$_m$ and CH$_p$ bonds (or 3-, 4-, and 5-positions). The intensities of these two aryl peaks were calculated for both the ⊥ and || conformers and an average was used. The experimentally determined local mode parameters for the CH$_o$ and CH$_{m,p}$ peaks from toluene-d_0[2] were used for both conformers.

In our previous papers on toluene-d_0 and -α-d_1, we found that the total intensity of the methyl region could be found by a very simple approach.[1,2] The anharmonicity of an α-CH oscillator changes by approximately 1 cm^{-1} between the ⊥ and || conformers. Such a change in anharmonicity leads to a very small change in intensity. Furthermore, coupling between CH bonds that share a common carbon atom is primarily important for the intensity of local mode combination bands, which do not carry significant intensity for $\Delta v_{CH} > 2$. Thus, if this coupling is neglected as well, the total methyl band intensity can be obtained from a simple one-dimensional model of an isolated rotating α-CH oscillator. The only difference between toluene-α-d_2, -α-d_1, and -d_0 is in the number of rotating α-CH oscillators which increases from 1 to 2 to 3, and is used as a multiplier to obtain the total methyl intensity.

Whereas the method described above is a suitable method to obtain total methyl intensities, it cannot be used to describe the methyl band profile. To simulate the methyl band profiles, we have added terms to the Hamiltonian to account for CH sretch−stretch coupling and CH stretch−torsion coupling.[19] The model approximates the frequency and anharmonicity dependence of the α-CH oscillator with torsional angle by[19]

$$\tilde{\omega}(\theta) = \tilde{\omega} + \delta_{\omega} \sin^2 \theta \tag{4}$$

with $\tilde{\omega} = \tilde{\omega}(\|)$ (the frequency of the α-CH oscillator in the

$$\tilde{\omega}x(\theta) = \tilde{\omega}x + \delta_{\omega x} \sin^2 \theta \tag{5}$$

|| position) and $\delta_{\omega} = \tilde{\omega}(\perp) - \tilde{\omega}(\|)$, and similar definitions for $\tilde{\omega}x$. This introduces coupling between the torsional and CH stretching modes. The pure torsional Hamiltonian is a rigid rotor with a small V_6 potential. The coupling between α-CH oscillators is approximated by harmonic coupling within the HCAO local mode model. Thus, the CH stretching torsional Hamiltonian for the methyl group in toluene can be written

$$\begin{aligned}(H_{\text{methyl}} - E_0)/hc = &\sum_{i=1}^{3}[v_i\tilde{\omega} - (v_i^2 + v_i)\tilde{\omega}x] + \\ &\sum_{i=1}^{3}\left[\left(v_i + \frac{1}{2}\right)\delta_{\omega} - \left(v_i + \frac{1}{2}\right)\delta_{\omega x}\right]\sin^2\theta_i + \\ &Bm^2 + \frac{V_6}{2}(1 - \cos 6\theta) - \\ &\gamma'(a_1a_2^+ + a_1^+a_2 + a_1a_3^+ + a_1^+a_3 + a_2a_3^+ + a_2^+a_3)\end{aligned} \tag{6}$$

where E_0 is the θ independent energy of the vibrational ground state, $\theta_1 = \theta$, $\theta_2 = \theta + 2\pi/3$, $\theta_3 = \theta - 2\pi/3$, B is the rotational constant for the methyl group, V_6 the torsional barrier, and γ' is the CH stretch−stretch coupling constant. The indices refer to the three α-CH oscillators.

Only small differences in this Hamiltonian arise for the different deuterated toluenes. For toluene-d_0, all terms in eq 6 are kept and the rotational constant is for a CH_3 group. To describe toluene-α-d_1, only two α-CH oscillators are included in the model, all terms with subscript 3 are removed, and B is calculated for a CH_2D group. Finally, toluene-α-d_2 has only one α-CH oscillator and the Hamiltonian is obtained by removing all terms with indices 2 and 3. B is calculated for a CHD_2 group. We neglect CH stretch−CD stretch coupling, which is small.

In the simple approach of calculating total methyl band intensities, the isolated rotating α-CH oscillator is described by the Morse oscillator Hamiltonian eq 3, with $\tilde{\omega}$ and $\tilde{\omega}x$ values determined from optimization of the methyl band profile simulations. The eigenstates in the more extended Hamiltonian of eq 6, which are used to simulate the methyl band profile, are products of Morse oscillator wave functions (one for each of the α-CH bonds) and real rigid rotor functions[19] (essentially $\cos(m\theta)$ and $\sin(m\theta)$ where m is the torsional quantum number). In the Hamiltonian of eq 6 we invoke an adiabatic separation of the torsional and CH stretching vibrations. Thus, we first solve the vibrational problem, i.e., the first and last terms in the Hamiltonian eq 6. This is done within the usual HCAO local mode approach.[5,13] An effective torsional potential will thus be generated for each of the vibrational eigenfunctions and the torsional eigenstates are found with this effective potential. As v increases, the vibrational energy increases and we would expect the adiabatic approximation to improve. We have compared this adiabatic approximation with a nonadiabatic approach in which the full Hamiltonian of eq 6 is diagonalized in the vibrational−torsional basis.

Dipole Moment Function. For an isolated CH oscillator, we express the dipole moment function as a series expansion in the internal CH displacement coordinate, q.

$$\vec{\mu}(q) = \sum_i \vec{\mu}_i q^i \tag{7}$$

where the coefficient $\vec{\mu}$ is $1/i!$ times the ith order derivative of the dipole moment function with respect to q. The dipole derivatives are found from ab initio calculated one-dimensional grids of the molecular dipole moment as a function of q with standard numerical techniques.[28] Compared to our previous work on toluene-d_0 and -α-d_1, we have increased the number of terms included in eq 7 to sixth-order from fourth-order, increased the number of points in the grid to nine from seven, and reduced the step size from 0.1 to 0.05 Å. We have recently found that these extensions slightly improve intensities for higher v.[29] (Similarly, larger grids and smaller step sizes are important in mapping the potential to obtain calculated values for the local mode frequency and anharmonicity.[30]) All grid points and the optimized geometries (⊥ and || conformers) have been calculated with Gaussian 94.[31] We have used the Hartree−Fock (HF) level of theory and the 6-311+G(d,p) basis set in all the ab initio calculations, as previous work has suggested that this method provides good agreement with observed absolute overtone intensities.[32,33]

The expansion coefficients of eq 7 for the aryl and methyl CH bonds in toluene are given in Table 1. Within the Born−Oppenheimer approximation, the toluenes will have the same dipole moment function. The dipole moment coefficients for the aryl CH bonds were calculated for both the ⊥ and || conformers. Very little difference was found between the two conformers and only the coefficients for the ⊥ conformer are given in Table 1. The coefficients were also calculated for a methyl CH bond in both the || position ($\theta = 0°$) and the ⊥ conformer ($\theta = 90°$). We have shown previously[2] that the variation of the α-CH dipole moment function with θ can to a good approximation be written

$$\vec{\mu}^x = \sum_i a_i \cos(\theta)\, q^i \tag{8}$$

where the coefficients a, b, c, and d can be determined from

$$\vec{\mu}^y = \sum_i b_i \sin(\theta)\, q^i \tag{9}$$

TABLE 1: Ab Initio HF/6-311+G(d,p) Dipole Moment Derivative Expansion Coefficients for Aryl and Methyl CH Bonds in Toluene[a]

$\vec{\mu}$	x/y[b]	z	bond
$\vec{\mu}_1$/D Å^{-1}	0.516	−0.330	CH_o
$\vec{\mu}_2$/D Å^{-2}	1.021	−0.539	CH_o
$\vec{\mu}_3$/D Å^{-3}	0.166	−0.0340	CH_o
$\vec{\mu}_4$/D Å^{-4}	0.229	−0.164	CH_o
$\vec{\mu}_5$/D Å^{-5}	−0.592	0.333	CH_o
$\vec{\mu}_6$/D Å^{-6}	−1.093	0.963	CH_o
$\vec{\mu}_1$/D Å^{-1}	−0.509	0.332	CH_m
$\vec{\mu}_2$/D Å^{-2}	−1.054	0.652	CH_m
$\vec{\mu}_3$/D Å^{-3}	−0.129	0.0730	CH_m
$\vec{\mu}_4$/D Å^{-4}	−0.252	0.150	CH_m
$\vec{\mu}_5$/D Å^{-5}	0.571	−0.331	CH_m
$\vec{\mu}_6$/D Å^{-6}	1.462	−1.225	CH_m
$\vec{\mu}_1$/D Å^{-1}	−0.119	0.599	CH_p
$\vec{\mu}_2$/D Å^{-2}	−0.0231	1.258	CH_p
$\vec{\mu}_3$/D Å^{-3}	−0.00230	0.142	CH_p
$\vec{\mu}_4$/D Å^{-4}	−0.00765	0.300	CH_p
$\vec{\mu}_5$/D Å^{-5}	0.00799	−0.620	CH_p
$\vec{\mu}_6$/D Å^{-6}	0.233	−1.959	CH_p
$\vec{\mu}_1$/D Å^{-1}	−0.628	−0.560	α-$CH_{\|\|}$
$\vec{\mu}_2$/D Å^{-2}	−0.890	−0.783	α-$CH_{\|\|}$
$\vec{\mu}_3$/D Å^{-3}	−0.0679	−0.142	α-$CH_{\|\|}$
$\vec{\mu}_4$/D Å^{-4}	−0.291	0.237	α-$CH_{\|\|}$
$\vec{\mu}_5$/D Å^{-5}	0.926	0.291	α-$CH_{\|\|}$
$\vec{\mu}_6$/D Å^{-6}	0.740	−0.566	α-$CH_{\|\|}$
$\vec{\mu}_{11}$/D Å^{-2}	−0.340	0.561	α-$CH_{\|\|}$
$\vec{\mu}_1$/D Å^{-1}	−0.594	−0.550	α-$CH_\perp$
$\vec{\mu}_2$/D Å^{-2}	−1.059	−1.158	α-$CH_\perp$
$\vec{\mu}_3$/D Å^{-3}	−0.204	−0.382	α-$CH_\perp$
$\vec{\mu}_4$/D Å^{-4}	−0.345	0.100	α-$CH_\perp$
$\vec{\mu}_5$/D Å^{-5}	1.114	0.780	α-$CH_\perp$
$\vec{\mu}_6$/D Å^{-6}	0.600	−0.0726	α-$CH_\perp$
$\vec{\mu}_{11}$/D Å^{-2}	−0.318	0.316	α-$CH_\perp$

[a] The indices refer to the order of the expansion coefficient. [b] For the CH_p and the α-$CH_\perp$ it is the *y* component. The *x* component is zero. For the other bonds it is the *x* component, and the *y* component is either zero or very small due to the fact that the ring is almost in the *yz* plane.

$$\vec{\mu}^z = \sum_i (c_i + d_i \cos(2\theta)) q^i \qquad (10)$$

the α-CH dipole moment coefficients that are calculated at the || [$\vec{\mu}_i$(||)] and ⊥ [$\vec{\mu}_i$(⊥)] positions and are defined by $a_i = \vec{\mu}_i^x(||)$, $b_i = \vec{\mu}_i^y(\perp)$, $c_i = {}^1/_2[\vec{\mu}_i^z(||) + \vec{\mu}_i^z(\perp)]$, and $d_i = {}^1/_2[\vec{\mu}_i^z(||) - \vec{\mu}_i^z(\perp)]$ with $\vec{\mu}_i(\perp)$ and $\vec{\mu}_i(||)$ given in Table 1.

Not surprisingly, the dipole derivatives in Table 1 are in good agreement with our previous calculations. The small differences for higher order terms arise from the change in grid size and step size in the dipole moment grid.[2] As in our previous papers,[1,2] we calculate the total intensity of an α-CH oscillator by averaging over the methyl torsion. Simple integration from 0 to $\pi/2$ and normalization over the four dipole components in eqs 8−10 gives $2/\pi$ [cos(θ) and sin(θ)], 1 (constant), and 0 [cos(2θ)]. These integration constants have to be included in eq 2 for the intensity calculation of a rotating α-CH oscillator. The total intensity of the different toluenes is then calculated as the sum of the number of rotating average α-CH bonds.

Methyl profile simulation requires a more complicated dipole moment function than does methyl intensity calculation. The dipole moment function used to simulate the methyl bands has additional terms for multiple α-CH oscillators and is identical in form to the one we used previously in our 2,6-difluorotoluene work.[19] (However, in ref 19 the definitions of *c* and *d* are reversed, and there is a typographical error in eq 20 of that paper; the signs should be reversed.) We refer to ref 19 for the full expressions of the dipole moment function. In summary the *x* component can be written

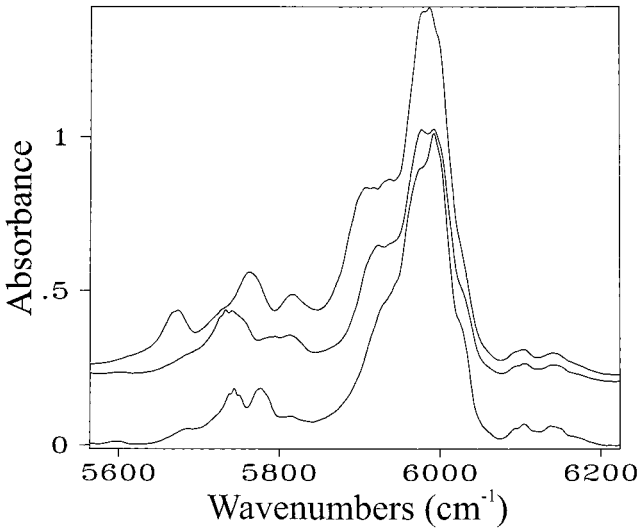

Figure 1. Room-temperature vapor phase overtone spectra of toluene-d_0 (top), -α-d_1 (middle), and -α-d_2 (bottom) in the $\Delta v_{CH} = 2$ region. The -d_0 and -α-d_1 spectra are taken from refs 2 and 1 and have been offset for clarity. The -α-d_2 spectrum was measured with a path length of 11.25 m and a pressure of 17 Torr.

$$\vec{\mu}^x(q^1,q_2,q_3,\theta) = \sum_{ijk}\sum_n \vec{\mu}^x_{ijkn} q_1^i q_2^j q_3^k \cos(n\theta + \text{phase}) \qquad (11)$$

where the phase is either 0 or $\pm 2\pi/3$, and similarly for the *y* and *z* component. The expansion is limited to the fourth-order diagonal and second-order mixed terms in the CH stretching coordinate, and to the constant and first nonzero term in the torsional coordinate. Again the necessary coefficients can be determined from the dipole moment grid that is calculated for the α-CH oscillator in the ⊥ and || positions. To determine the mixed (e.g., q_1, q_2) terms, a symmetric two-dimensional grid had to be calculated.[13] We used a 9 × 9 grid with a 0.05 Å stepsize. The second-order mixed dipole terms $\vec{\mu}_{11}$ are also given in Table 1. We have calculated these terms for the two CH bonds opposite to the bond in either the || or ⊥ position. The methyl dipole moment functions used in the methyl band profile simulation are identical for both the adiabatic and nonadiabatic methods.

In the same manner as for the Hamiltonian, terms in the dipole moment function of eq 11 with respect to one α-CH coordinate are deleted for the toluene-α-d_1 simulation, and with respect to two α-CH coordinates for the toluene-α-d_2 simulations.

Results and Discussion

The room-temperature vapor phase overtone spectrum of toluene-α-d_2 in the CH stretching regions corresponding to $\Delta v_{CH} = 2-6$ is shown in Figures 1−5. The overtone spectra of toluene-d_0[2] and toluene-α-d_1[1] from our previous work are also shown for comparison and have been offset for clarity. The aryl region of the spectrum is virtually identical in all three molecules, except at $\Delta v_{CH} = 2$. The small changes in the low-energy side of the aryl peak at $\Delta v_{CH} = 2$ (Figure 1) are due to differences in methyl local mode combination peaks.[1] For $\Delta v_{CH} = 3-6$, the aryl region of the spectrum of toluene-α-d_2 has been decomposed into two peaks that correspond to the longer ortho CH bond at lower frequency and the shorter meta and para CH bonds at higher frequency. In Table 2, we give the observed frequencies of the two aryl peaks ($\Delta v_{CH} = 3-6$) as well as the relative areas of the two aryl peaks and the methyl

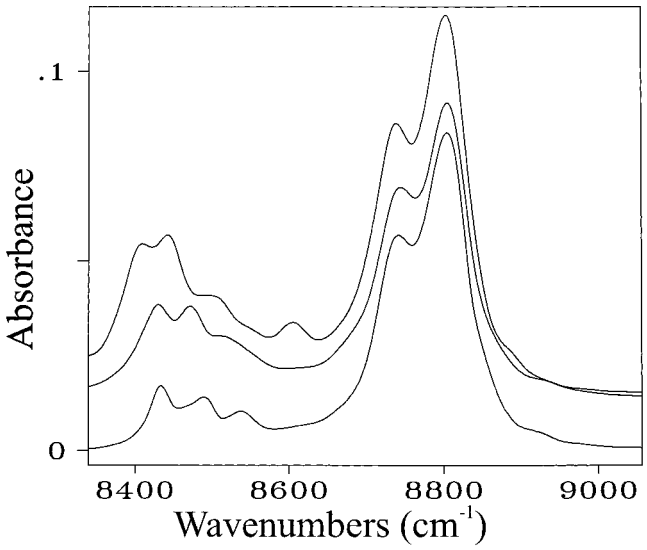

Figure 2. Room-temperature vapor phase overtone spectra of toluene-d_0 (top), -α-d_1 (middle), and -α-d_2 (bottom) in the $\Delta v_{CH} = 3$ region. The -d_0 and -α-d_1 spectra are taken from refs 2 and 1 and have been offset for clarity. The -α-d_2 spectrum was measured with a path length of 11.25 m and a pressure of 17 Torr.

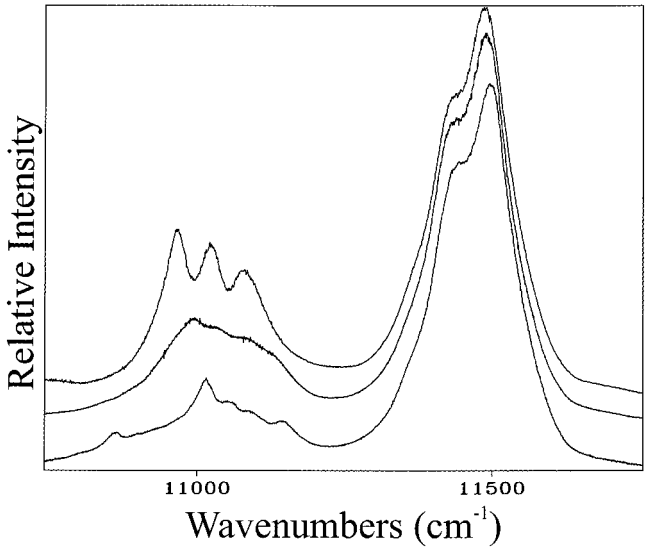

Figure 3. Room-temperature vapor phase overtone spectra of toluene-d_0 (top), -α-d_1 (middle), and -α-d_2 (bottom) in the $\Delta v_{CH} = 4$ region. The -d_0 and -α-d_1 spectra are taken from refs 2 and 1 and have been offset for clarity. All spectra were measured by ICL-PAS. The bottom spectrum corresponds to a sample pressure of 17 Torr of toluene-α-d_2 and 97 Torr of argon buffer gas.

band. Similar results are presented for the toluene-α-d_1 and -d_0 molecules from our previous work.[1,2]

The observed frequencies $\tilde{\nu}$ of the aryl local mode peaks have been fitted to a two-parameter Morse oscillator expression

$$\tilde{\nu}/v = \tilde{\omega} - (v + 1)\tilde{\omega}x \qquad (12)$$

to obtain values for the local mode frequency $\tilde{\omega}$ and anharmonicity $\tilde{\omega}x$ for the two aryl CH oscillators. These parameters are reported in Table 3. As expected, the values are identical for the three molecules, within the small uncertainties. We use the values for toluene-d_0 in all calculations of intensities and in the simulations.

The corresponding parameters for the methyl group were not obtained on the basis of a Birge−Sponer analysis. Rather these parameters were obtained as part of the procedure that we used

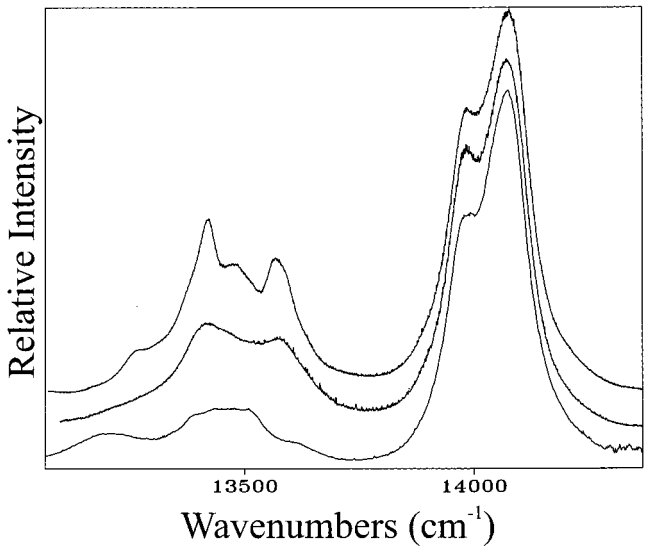

Figure 4. Room-temperature vapor phase overtone spectra of toluene-d_0 (top), -α-d_1 (middle), and -α-d_2 (bottom) in the $\Delta v_{CH} = 5$ region. The -d_0 and -α-d_1 spectra are taken from refs 2 and 1 and have been offset for clarity. All spectra were measured by ICL-PAS. The bottom spectrum corresponds to a sample pressure of 17 Torr of toluene-α-d_2 and 95 Torr of argon buffer gas.

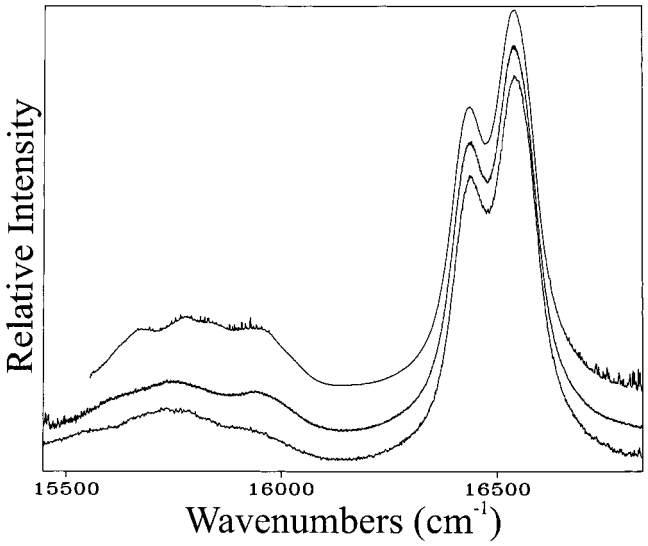

Figure 5. Room-temperature vapor phase overtone spectra of toluene-d_0 (top), -α-d_1 (middle), and -α-d_2 (bottom) in the $\Delta v_{CH} = 6$ region. The -d_0 and -α-d_1 spectra are taken from refs 2 and 1 and have been offset for clarity. All spectra were measured by ICL-PAS. The bottom spectrum corresponds to a sample pressure of 17 Torr of toluene-α-d_2. The methyl region of the spectrum was recorded with the dye DCM and 95 Torr of argon buffer gas. The aryl region of the spectrum was recorded with the dye R6G and 88 Torr of argon buffer gas.

to simulate the complex methyl regions of the overtone spectra (see the preceding section on Theory and Calculations). We use local mode parameters from ab initio calculations as a first approximation.[30] However, since ab initio frequencies at the HF/6-311+G(d,p) level are often overestimated, appropriate scaling factors are required. We calculate methyl scaling factors for *trans*-2-butene and 2,3-dimethylbutadiene, as their experimental values are known[10,34] and the methyl environments are similar to that in toluene. At the HF/6-311+G(d,p) level we obtain the scaling factors 0.9474 for frequency and 0.967 for anharmonicity. The scaled ab initio parameters for toluene are listed in Table 4. We use the HCAO local mode model to calculate the methyl spectral profiles. The rotational constant B (in cm^{-1}) of

TABLE 2: Observed and Calculated Relative Intensities, Observed Frequencies and Peak Assignments for the CH Stretching Overtone Spectra of Vapor Phase Toluene-α-d_2, -α-d_1, and -d_0

	toluene α-d_2			toluene α-d_1		toluene-d_0	
$\tilde{\nu}$/cm^{-1}	f_{obs}[a]	f_{calc}[b]	assignt	f_{obs}[c]	f_{calc}[b]	f_{obs}[d]	f_{calc}[b]
	(0.56)	0.55	$\|3\rangle_\alpha$	(1.1)	1.09	(1.4)	1.64
8737	(1.0)	1.0	$\|3\rangle_o$	(1.0)	1.0	(1.0)	1.0
8804	(1.7)	1.95	$\|3\rangle_{m,p}$	(1.3)	1.95	(1.4)	1.95
	0.59 (0.45)	0.50	$\|4\rangle\alpha$	0.89 (1.1)	1.00	1.2 (1.4)	1.50
11431	1.0 (1.0)	1.0	$\|4\rangle_o$	1.0 (1.0)	1.0	1.0 (1.0)	1.0
11501	1.5 (2.3)	1.98	$\|4\rangle_{m,p}$	1.5 (1.6)	1.98	1.5 (2.1)	1.98
	1.0	0.47	$\|5\rangle\alpha$	1.4	0.93	1.6	1.40
13977	1.0	1.0	$\|5\rangle_o$	1.0	1.0	1.0	1.0
14073	2.7	1.94	$\|5\rangle_{m,p}$	1.9	1.94	1.8	1.94
	0.93	0.56	$\|6\rangle\alpha$	0.8	1.13	1.4	1.69
16434	1.0	1.0	$\|6\rangle_o$	1.0	1.0	1.0	1.0
16546	2.1	1.87	$\|6\rangle_{m,p}$	2.1	1.87	1.9	1.87

[a] Ratios in parentheses are from Cary spectra. [b] Calculated with the HF/6-311+G(d,p) dipole moment function and the local mode parameters in Tables 3 (toluene-d_0) and 4 (best fit $\tilde{\omega}$ and $\tilde{\omega}x$). [c] From ref 1. [d] From ref 2.

TABLE 3: Local Mode Frequency and Anharmonicity of the Aryl CH Stretching Modes in Vapor Phase Toluene-α-d_2, -α-d_1, and -d_0[a]

	toluene-α-d_2[b]	toluene-α-d_1[c]	toluene-d_0[d]
$\tilde{\omega}$ (CH$_o$)/cm^{-1}	3146 ± 5	3146 ± 2	3144 ± 2
$\tilde{\omega}$ (CH$_{m,p}$)/cm^{-1}	3171 ± 3	3169 ± 3	3170 ± 2
$\tilde{\omega}x$ (CH$_o$)/cm^{-1}	58.2 ± 0.8	58.2 ± 0.3	57.9 ± 0.3
$\tilde{\omega}x$ (CH$_{m,p}$)/cm^{-1}	59.2 ± 0.6	58.9 ± 0.4	59.1 ± 0.4

[a] Uncertainties are one standard deviation. [b] From a fit of the local mode frequencies in the $\Delta v_{CH} = 3-6$ regions. [c] From ref 1. [d] From ref 2.

TABLE 4: Methyl Parameters for the Overtone Spectra of Toluene-α-d_2, -α-d_1, and -d_0 (cm^{-1})[a]

	ab initio[b]	scaled ab initio[c]	best fit[d]
$\tilde{\omega}$ (α-CH)	3238	3068	3072
$\tilde{\omega}x$ (α-CH)	63.3	61.3	59
δ_ω	−39.7	−37.6	−36
$\delta_{\omega x}$	1.1	1.0	1.0

[a] The value of $V_6 = 4.9$ cm^{-1} is taken from ref 27. The value of the rotational constants are $B(CH_3) = 5.43$ cm^{-1}, $B(CH_2D) = 4.06$ cm^{-1}, and $B(CHD_2) = 3.27$ cm^{-1} and were determined from the ab initio optimized geometry. [b] At the HF/6-311+G(d,p) level. [c] Scaling factors determined from ab initio calculated frequencies and anharmonicities for *trans*-2-butene and 2,3-dimethylbutadiene. [d] See text.

the methyl group is calculated to be 5.43, 4.06, and 3.27 for CH_3, CH_2D, and CHD_2 at the ab initio optimized geometry. The B value is expected to decrease as the methyl CH oscillators are excited to higher CH stretching vibrational levels, and also to change with the torsion angle. However, these changes are not included in our model.

We use the adiabatic approximation that separates fast CH stretching motion from methyl torsional motion. Note that the variation of the CH stretching parameters with torsional angle creates a potential for torsion in addition to the V_6 potential. This effect has also been noted by Cavagnat and coworkers.[16-18] At first, we calculate the methyl overtone spectral profiles from $\Delta v_{CH} = 2-5$ with the scaled ab initio parameters shown in Table 4. Then only the $\tilde{\omega}$ parameter is changed, and another group of spectral profiles is obtained. In the same way, we change $\tilde{\omega}x$, δ_ω, and $\delta_{\omega x}$. We use the central frequency at half-maximum and the full width at half-maximum to characterize a spectral profile. We calculate the changes in these two

TABLE 5: Observed and Calculated Total Oscillator Strengths of the CH Stretching Regions in Vapor Phase Toluene-α-d_2, -α-d_1, and -d_0

v	obs (-α-d_2)	calc[a] (-α-d_2)	obs[b] (-α-d_1)	calc[a] (-α-d_1)	obs[c] (-d_0)	calc[a] (-d_0)
1		2.5×10^{-5}		3.1×10^{-5}		3.7×10^{-5}
2	5.2×10^{-7}	4.1×10^{-7}	4.7×10^{-7}	4.7×10^{-7}	5.6×10^{-7}	5.3×10^{-7}
3	5.8×10^{-8}	5.4×10^{-8}	6.2×10^{-8}	6.2×10^{-8}	6.7×10^{-8}	7.1×10^{-8}
4	3.1×10^{-9}	4.5×10^{-9}	3.6×10^{-9}	5.2×10^{-9}	4.0×10^{-9}	5.8×10^{-9}
5		7.1×10^{-10}		8.1×10^{-10}		9.0×10^{-10}

[a] Calculated with the local mode parameters of Tables 3 (toluene-d_0) and 4 (best fit $\tilde{\omega}$ and $\tilde{\omega}x$) and the HF/6-311+G(d,p) dipole moment function. [b] From ref 1. [c] From ref 2.

quantities caused by $\tilde{\omega}$, $\tilde{\omega}x$, δ_ω, and $\delta_{\omega x}$. Analysis of these changes indicates the direction to change the parameters.

The methyl profiles react differently to changes in the four parameters. Not surprisingly, the most important parameters for the central frequency are $\tilde{\omega}$ and $\tilde{\omega}x$, whereas the effects of δ_ω and $\delta_{\omega x}$ are insignificant. The uncertainty in $\tilde{\omega}x$ is much larger as a percentage than the uncertainty in $\tilde{\omega}$. If we change $\tilde{\omega}$ and $\tilde{\omega}x$ by an amount that corresponds to their uncertainties, the net effects on the central frequencies are comparable. The largest effect on the width comes from the δ_ω parameter with the other three parameters having small but not negligible effects. Thus, our analysis yields results that are intuitive. The $\tilde{\omega}$ and δ_ω parameters have the most significant effects on the central frequency and the width, respectively.

The last column of Table 4, labeled best fit, lists the parameters obtained on the basis of this procedure. Note that these parameters are obtained only on the basis of a comparison for toluene-d_0. $\tilde{\omega}$ and $\tilde{\omega}x$ from Table 4, along with the toluene-d_0 aryl parameters are used in subsequent calculations of overtone intensities for all three molecules.

The relative calculated oscillator strengths are given in Table 2 for all three molecules. The observed and calculated absolute total oscillator strengths are compared in Table 5 for those regions where we have conventional spectra ($\Delta v_{CH} = 2-4$). The total overtone intensities calculated with the HF/6-311+G-(d,p) dipole moment function are in good agreement with the observed intensities. Note also that the expected ratio of the total absolute intensities should be approximately 6:7:8 (1:1.17:1.33) for the toluene-α-d_2, -α-d_1, and -d_0 molecules if one assumes the same intensity contribution from methyl and aryl CH oscillators. The average calculated ratio for $\Delta v_{CH} = 2-5$ is 1:1.15:1.29 with a maximum deviation from the average value of 0.02.

The observed relative intensities in Table 2 all show the expected decrease in the methyl intensity relative to the aryl intensity from toluene-d_0 to -α-d_1 to -α-d_2. The decrease also appears in the absolute oscillator strengths in Table 5, although the observed value for $\Delta v_{CH} = 2$ for toluene-α-d_2 appears to be anomalously high. The calculated intensities reproduce the expected trend. On the basis of the Born−Oppenheimer approximation and the approach we have used in calculating methyl intensities, the methyl intensity should be in the ratio of 3:2:1 for the -d_0, -α-d_1, and -α-d_2 molecules.

The methyl intensities calculated with the simple isolated rotating α-CH oscillator model are in good agreement with methyl intensities that are obtained as the sum of all the vibrational−torsional transitions in the methyl band profile simulations. The agreement improves with increasing v_{CH} as the $\vec{\mu}_{11}$ term, which is included in the simulation, is more important for the lower overtones.[13]

The ratio of total aryl to total methyl intensities should minimize uncertainties introduced by our deconvolution pro-

TABLE 6: Observed and Calculated Aryl to Methyl Intensity Ratios in CH Stretching Overtone Spectra of Vapor Phase Toluene-α-d_2, -α-d_1, and -d_0

	toluene-α-d_2		toluene-α-d_1		toluene-d_0	
v	obs[a]	calc[b]	obs[a]	calc[b]	obs[a]	calc[b]
3	(4.8)	5.4	(2.1)	2.7	(1.7)	1.8
4	4.3 (7.3)	6.0	2.8 (2.3)	3.0	2.1 (2.1)	2.0
5	3.6	6.3	2.1	3.1	1.7	2.1
6	3.4	5.1	3.8	2.5	2.1	1.7

[a] Ratios in parentheses are from Cary spectra. [b] Local mode calculations from the parameters of Tables 3 (toluene-d_0) and 4 (best fit $\tilde{\omega}$ and $\tilde{\omega}x$) and the HF/6-311+G(d,p) dipole moment function.

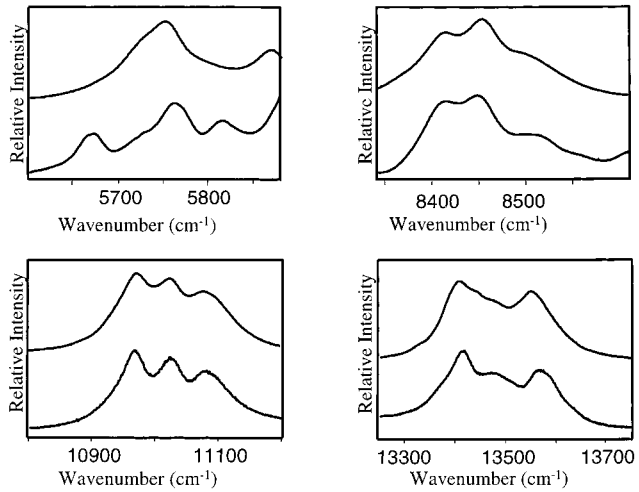

Figure 6. Observed (bottom) and simulated (top) spectra of toluene-d_0 in the methyl regions of $\Delta v_{CH} = 2-5$.

cedure. Observed and calculated values for this ratio are presented in Table 6. At $\Delta v_{CH} = 6$, the spectra were measured with two dyes. Thus, there is an additional source of error in the observed relative intensities in Table 2 and the observed aryl to methyl intensity ratio in Table 6, and the intensity data for toluene -α-d_2 at $\Delta v_{CH} = 6$ in Tables 2 and 6 should be regarded as an estimate. Because of the lower relative intensity of the methyl regions in the two deuterated molecules, the uncertainty becomes progressively higher in the ratio from -d_0 to -α-d_1 to -α-d_2. In all cases except for $\Delta v_{CH} = 6$ in -α-d_2, the observed aryl to methyl intensity ratio increases from -d_0 to -α-d_1 to -α-d_2. The methyl intensity is very sensitive to the location of the baseline, and this effect becomes increasingly important as the total methyl intensity decreases from -d_0 to -α-d_1 to -α-d_2. Thus, the observed intensity ratios in Table 6 for -α-d_2 are subject to larger uncertainties.

The biggest challenge in our current work is the attempt to simulate the methyl regions of the spectra of the three toluene molecules. The results of that simulation are shown in Figures 6−8 where we have compared the observed and simulated spectra for all three molecules from $\Delta v_{CH} = 2-5$. The observed methyl profiles differ in all three molecules. The toluene-d_0 methyl profile shows more structure than either -α-d_1 or -α-d_2. Both the -α-d_1 and -α-d_2 methyl profiles appear to broaden relative to -d_0 at $\Delta v_{CH} = 4$ and 5.

The difference in the methyl profiles between the three molecules provides strong evidence that torsional modes are actively coupled to the methyl CH stretching overtones. Both $\tilde{\omega}$ and $\tilde{\omega}x$ depend on the torsional angle (see eqs 4 and 5). It is this dependence on torsional angle that introduces an effective barrier to methyl rotation in the excited CH stretching states that increases with increasing v_{CH}. Thus, the wave functions

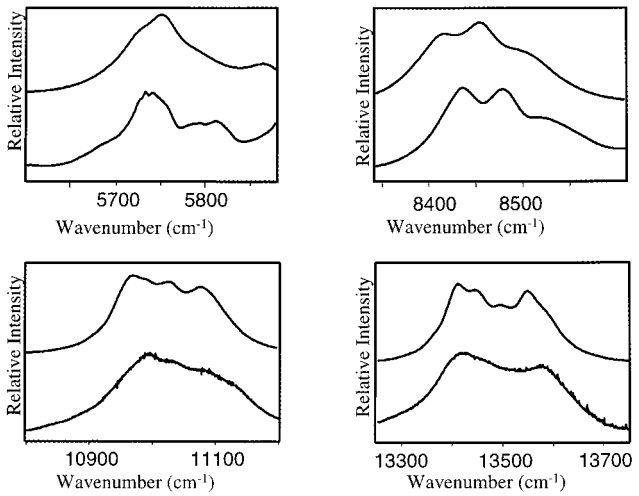

Figure 7. Observed (bottom) and simulated (top) spectra of toluene-α-d_1 in the methyl regions of $\Delta v_{CH} = 2-5$.

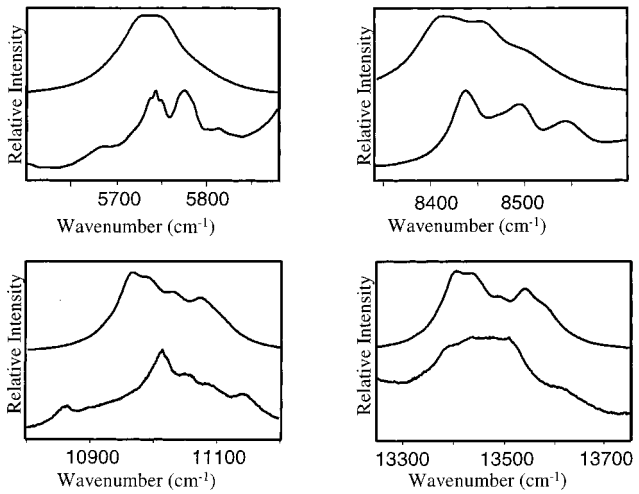

Figure 8. Observed (bottom) and simulated (top) spectra of toluene-α-d_2 in the methyl regions of $\Delta v_{CH} = 2-5$.

are localized in torsional minima in the excited CH stretching states, and this localization is essentially complete for $\Delta v_{CH} \geq 4$.[16−18]

Given the simplicity of the theory outlined in the Theory and Calculations section, it is surprising that the simulations in Figures 6−8 work as well as they do. Both the overall shape of the band and the change from molecule to molecule are in good agreement. The agreement for $\Delta v_{CH} = 2$ is not as good as for the other overtones. The lack of good agreement at $\Delta v_{CH} = 2$ is to be expected since combination bands that involve CH stretching and lower frequency normal modes appear in this region. Such combination bands are not included in the model. The rise at the high-frequency end of the observed spectra in Figures 6−8 at $\Delta v_{CH} = 2$ indicates the onset of the aryl CH absorption. For $\Delta v_{CH} = 3-5$ the agreement appears to diminish from toluene-d_0 to -α-d_1 to -α-d_2. Again, this is expected since the best fit parameters were found through comparison to the toluene-d_0 spectrum. These were the parameters that were used to simulate the methyl profiles for all three molecules.

In our work on the overtone spectrum of 2,6-difluorotoluene, we calculated the methyl profiles with a model that was based on a local mode treatment of the three methyl CH stretching modes and a simple one-dimensional rigid rotor for torsion. Just as in the current model, interaction between torsion and stretching occurred through angular-dependent terms in both

the frequency (δ_ω) and anharmonicity ($\delta_{\omega x}$) and angular dependent terms were also included in the dipole moment function. Because of the coupling between torsion and stretch in the Hamiltonian and in the dipole moment function, a very large number of transitions were predicted to carry intensity and to contribute to the overall spectral profile. That model differed from the model we have used in this work in that it did not invoke an adiabatic separation between torsion and stretching. Thus, a full diagonalization procedure was invoked to obtain the final set of vibrational states.

When we applied this nonadiabatic model with full diagonalization to toluene-d_0 we found that the results were largely independent of γ', the interoscillator coupling parameter. For the adiabatic model, agreement with the full model and with the observed profiles in toluene-d_0 occurred with $\gamma' = 0$. The full model gives good agreement with $\Delta v_{CH} = 3$, 4, and 5 in toluene-d_0. In the adiabatic model, the agreement is better for $\Delta v_{CH} = 4$ and 5 than it is for $\Delta v_{CH} = 3$. This observation is in accord with the expectation that the adiabatic approximation should improve as v_{CH} increases.

The comparison of the success of the adiabatic and nonadiabatic models for toluene-d_0, and the unimportance of γ' lead us to the conclusion that stretch−stretch coupling is negligible for higher overtones ($\Delta v_{CH} \geq 4$) in the presence of strong torsion−stretch coupling. In a classical picture one could consider three time scales. The time for methyl rotation and for CH stretching are two of these time scales. The difference between the faster stretching motion and the slower methyl rotation forms the basis for the adiabatic separation of these modes. The third time scale is the time it takes the CH stretching vibrational energy to transfer from one methyl CH bond to another. The inverse of the splitting between the symmetrized pure local mode CH stretching states is a measure of that time. For $v_{CH} \geq 3$ the splitting between symmetrized pure local mode states is very small for a given v_{CH}, and becomes even smaller as v_{CH} increases. When the time scale for CH stretching energy transfer from one CH bond to another is comparable or longer than the time scale for methyl rotation, torsion−stretch coupling will dominate and stretch−stretch coupling will be insignificant.

Conclusion

We have used conventional and intracavity laser photoacoustic spectroscopy to measure the vapor phase overtone spectrum of toluene-α-d_2 in the region corresponding to $\Delta v_{CH} = 2-6$. Oscillator strengths have been measured absolutely for $\Delta v_{CH} = 2-4$. For $\Delta v_{CH} = 2-6$, the relative oscillator strengths of the two aryl peaks and of the methyl band were also measured.

We have used a model similar to the one used for our previous work on toluene-d_0[2] and toluene-α-d_1[1] to calculate the intensities of the CH stretching aryl and methyl transitions. The calculations yield results that are in good agreement with observations for both absolute and relative intensities.

Whereas the aryl regions of the overtone spectra are essentially identical for all three molecules, the methyl region changes both in relative intensity, as expected, and in the shape of the methyl profile. These methyl profiles have been successfully simulated on the basis of a simple adiabatic model. The model incorporates changes in stretching frequency and anharmonicity with torsional angle. Vibrational states are generated from an HCAO local mode approach. A dipole moment function is obtained from ab initio calculations and includes dependence on both CH stretching coordinates and torsional angle. The model accounts well for the change in methyl profile between the three molecules. Comparison of our model to a nonadiabatic model, and the observed unimportance of γ' within the adiabatic model, demonstrate that torsion−stretch coupling is dominant for higher overtones ($\Delta v_{CH} \geq 4$) and that stretch−stretch coupling is negligible.

Acknowledgment. B.R.H. is grateful to the University of Otago for providing office facilities during a visit. We are grateful to Michael W. P. Petryk for help with the deconvolutions. Funding for this research has been provided by the Natural Sciences and Engineering Research Council of Canada and by the University of Otago. Z.R. is grateful to the University of Otago for a Specified Research Scholarship.

References and Notes

(1) Kjaergaard, H. G.; Turnbull, D. M.; Henry, B. R. *J. Phys. Chem. A* **1998**, *102*, 6095.
(2) Kjaergaard, H. G.; Turnbull, D. M.; Henry, B. R. *J. Phys. Chem. A* **1997**, *101*, 2589.
(3) Hayward, R. J.; Henry, B. R. *J. Mol. Spectrosc.* **1975**, *57*, 221.
(4) Henry, B. R. *Acc. Chem. Res.* **1977**, *10*, 207.
(5) Mortensen, O. S.; Henry, B. R.; Mohammadi, M. A. *J. Chem. Phys.* **1981**, *75*, 4800.
(6) Child, M. S.; Lawton, R. T. *Faraday Discuss. Chem. Soc.* **1981**, *71*, 273.
(7) Sage, M. L.; Jortner, J. *Adv. Chem. Phys.* **1981**, *47*, 293.
(8) Child, M. S.; Halonen, L. *Adv. Chem. Phys.* **1984**, *57*, 1.
(9) Kjaergaard, H. G.; Henry, B. R. *J. Phys. Chem.* **1995**, *99*, 899.
(10) Turnbull, D. M.; Kjaergaard, H. G.; Henry, B. R. *Chem. Phys.* **1995**, *195*, 129.
(11) Kjaergaard, H. G.; Henry, B. R. *J. Chem. Phys.* **1992**, *96*, 4841.
(12) Kjaergaard, H. G.; Turnbull, D. M.; Henry, B. R. *J. Chem. Phys.* **1993**, *99*, 9438.
(13) Kjaergaard, H. G.; Henry, B. R.; Tarr, A. W. *J. Chem. Phys.* **1991**, *94*, 5844.
(14) Reddy, K. V.; Heller, D. F.; Berry, M. J. *J. Chem. Phys.* **1982**, *76*, 2814.
(15) Gough, K. M.; Henry, B. R. *J. Phys. Chem.* **1984**, *88*, 1298.
(16) Cavagnat, D.; Lespade, L.; Lapouge, C. *J. Chem. Phys.* **1995**, *103*, 10502.
(17) Lapouge, C.; Cavagnat, D. *J. Phys. Chem. A* **1998**, *102*, 8393.
(18) Cavagnat, D.; Lespade, L. *J. Chem. Phys.* **1997**, *106*, 7946.
(19) Zhu, C.; Kjaergaard, H. G.; Henry, B. R. *J. Chem. Phys.* **1997**, *107*, 691.
(20) Proos, R. J.; Henry, B. R. *J. Phys. Chem. A* **1999**, *103*, 8762.
(21) Petryk, M. W. P. M.Sc. thesis, University of Guelph, 1998.
(22) Cavagnat, D.; Lascombe, J. *J. Chem. Phys.* **1982**, *76*, 4336.
(23) Atkins, P. W. *Molecular Quantum Mechanics*, 2nd ed.; Oxford University: Oxford, U.K., 1983.
(24) Henry, B. R.; Sowa, M. G. *Prog. Anal. Spectrosc.* **1989**, *12*, 349.
(25) Henry, B. R.; Kjaergaard, H. G.; Niefer, B.; Schattka, B. J.; Turnbull, D. M. *Can. J. Appl. Spectrosc.* **1993**, *38*, 42.
(26) Spectra Calc is a commercially available product from Galactic Industries Corp. Marquardt's nonlinear least-squares fiting algorithm is used: Marquardt, D. W. *J. Soc. Ind. Appl. Math.* **1963**, *11*, 431.
(27) Kreiner, W. A.; Rudolph, H. D.; Tan, B. *J. Mol. Spectrosc.* **1973**, *48*, 86.
(28) Press, W. H.; Flannery, B. F.; Teukolsky, S. A.; Vetterling, W. T. *Numerical Recipes in C*; Cambridge University: Cambridge, U.K., 1988.
(29) Daub, C. D.; Henry, B. R.; Sage, M. L.; Kjaergaard, H. G. *Can. J. Chem.* **1999**, *77*, 1775.
(30) Low, G. R.; Kjaergaard, H. G. *J. Chem. Phys.* **1999**, *110*, 9104.
(31) Frisch, M. J.; Trucks, G. W.; Schlegel, H. B.; Gill, P. M. W.; Johnson, B. G.; Robb, M. A.; Cheeseman, J. R.; Keith, T.; Petersson, G. A.; Montgomery, J. A.; Raghavachari, K.; Al-Laham, M. A.; Zakrzewski, V. G.; Ortiz, J. V.; Foresman, J. B.; Cioslowski, J.; Stefanov, B. B.; Nanayakkara, A.; Challacombe, M.; Peng, C. Y.; Ayala, P. Y.; Chen, W.; Wong, M. W.; Andres, J. L.; Replogle, E. S.; Gomperts, R.; Martin, R. L.; Fox, D. J.; Binkley, J. S.; Defrees, D. J.; Baker, J.; Stewart, J. P.; Head-Gordon, M.; Gonzalez, C.; Pople, J. A. *Gaussian94*, Revision D.4; Gaussian, Inc.: Pittsburgh, PA, 1995.
(32) Kjaergaard, H. G.; Henry, B. R. *Mol. Phys.* **1994**, *83*, 1099.
(33) Kjaergaard, H. G.; Daub, C. D.; Henry, B. R. *Mol. Phys.* **1997**, *90*, 201.
(34) Fang, H. L.; Compton, D. A. C. *J. Phys. Chem.* **1988**, *92*, 7185.